

Org. Commun. XX:X (2025) X-XX

organic communications

# Synthesis and antidiabetic assessment of substituted 2-benzylidene-1-indanone derivatives using *in vitro* and *in silico* techniques

Selvakumar Sabapathi <sup>1</sup>, Babai Mahdi <sup>1</sup>, Mohamad Hafizi Abu Bakar <sup>3</sup>, Andrey A. Mikhaylov <sup>4,5</sup>, Mohammad Tasyriq Che Omar <sup>6</sup>, Azeana Zahari <sup>7</sup>, S. Yaallini Sukumaran <sup>7</sup> and Mohamad Nurul Azmi <sup>1</sup>,

<sup>1</sup>School of Chemical Sciences, Universiti Sains Malaysia, 11800 Minden, Penang, Malaysia <sup>2</sup>Department of Chemistry, Nigerian Army University Biu, Borno State, 1500, Nigeria <sup>3</sup>School of Industrial Technology, Universiti Sains Malaysia, 11800 Minden, Penang, Malaysia <sup>4</sup>Shemyakin-Ovchinnikov Institute of Bioorganic Chemistry of the Russian Academy of Sciences, 16/10 Miklukho-Maklaya St, Moscow 117997, Russia

 <sup>5</sup>Laboratory of Medicinal Substances Chemistry, Institute of Translational Medicine, Pirogov Russian National Research Medical University, Ostrovitianov 1, Moscow, 117997, Russia
 <sup>6</sup>School of Distance Education, Universiti Sains Malaysia, 11800 Minden, Penang, Malaysia
 <sup>7</sup>Department of Chemistry, Faculty of Science, University of Malaya, 50603 Kuala Lumpur, Malaysia

(Received August 31, 2025; Revised October 27, 2025; Accepted October 28, 2025)

Abstract: In search for novel antidiabetic agents, a new series of substituted 2-benzylidene-1-indanone derivatives were synthesized via crossed Adol condensation reaction. The structures of the synthesized compounds were determined using various spectroscopic techniques, including HREIMS, FTIR, and NMR. The enzyme inhibitory activities of the target analogues were assessed using in vitro assays. The tested compounds demonstrated inhibitory potential against α-amylase, as indicated by their IC<sub>50</sub> values ranging from 17.7 to 28.2 μM as compared to standard drug acarbose with IC<sub>50</sub> value of  $30.2 \pm 1.9 \mu M$ . Furthermore, molecular docking study was conducted to elucidate the binding interactions of the compounds within the  $\alpha$ -amylase enzyme binding pocket (PDB ID 2QV4). The results of molecular docking studies indicated that compounds 3m, 3c, 3d has the lowest binding energy (-9.8, -9.3 and -9.4, respectively). The structure-activity relationship (SAR) analysis revealed that alteration in the inhibitory activities of  $\alpha$ -amylase enzymes was provided by distinct types of substituents attached to either *ortho*- or *para* positions of the phenyl group. The combined SAR and docking results highlight the importance of para-position substitution on ring A for optimal activity, particularly when introducing moderately electron-withdrawing groups such as chlorine, fluorine, and bromine. Thus, in the pursuit of developing newer antidiabetic agents, the in silico ADME prediction was carried out with promising physicochemical, drug likeness and ADME properties which indicated that some compounds were considered drug-like as they do not violate any of the rule-based filters of Lipinski.

**Keywords:** 2-benzylidene-1-indanone derivatives; Aldol condensation reaction;  $\alpha$ -amylase inhibitor; molecular docking; ADME properties. ©2025 ACG Publication. All right reserved.

## 1. Introduction

A variety of metabolic diseases brought on by different pathogenic pathways are included in diabetes mellitus, and they are all characterized by hyperglycemia. It is among the world's most common

<sup>\*</sup> Corresponding author: E-Mail: mnazmi@usm.my

health issues. Nowadays, there are more adult-onset diabetes cases worldwide, which motivates researchers to find effective novel treatments. Diabetes affects a person's quality of life and functional capacities. It also contributes to high rates of morbidity and early death, which is a growing medical and public health concern.<sup>2</sup> There were 463 million cases of diabetes worldwide in 2019.<sup>3</sup> The most prevalent type of diabetes is type II, which develops when the body either stops producing enough insulin or becomes resistant to it, making it difficult to successfully control blood glucose levels.<sup>4,5</sup> However, Type I diabetes generally manifests in childhood and is caused by the immune system targeting and killing the pancreatic cells that produce insulin.<sup>6,7</sup> Type 2 diabetes mellitus (T2DM) is becoming more and more common worldwide, despite improvements in diabetes care. About 415 million persons worldwide have diabetes in 2015, according to the International Diabetes Federation (IDF), with 20% of those instances occurring in Southeast Asia. By 2040, this figure is expected to rise to 642 million.8 Based on data from the National Health and Morbidity Survey (NHMS), the prevalence of type 2 diabetes in Malaysia increased dramatically from 6.3% in 1986 to 17.5% in 2015. According to research, there will be between 13.5 and 17.4 million instances of type 1 diabetes (T1D) worldwide by 2040, which is a 60% to 107% rise from 2021. 10 Recent studies showed that people under 60 account for more than one-third of diabetesrelated fatalities.11

Increased consumption of poor foods and sedentary lifestyles, which raise body mass index (BMI) and fasting plasma glucose levels, have been linked to the rising prevalence of diabetes. <sup>12</sup> Type 2 diabetes, which affects over 90% of diabetics, is impacted by genetic, environmental, demographic, and socioeconomic variables.<sup>13</sup> Besides, gestational diabetes also tends to develop into T2D and cardiovascular disease after pregnancy which is also characterized by chronic insulin resistance. However, there is limited information on the role of A1 and A2A ARs in T2D.<sup>14</sup> Urbanization, population aging, a decrease in physical activity, and an increase in overweight and obesity are major factors contributing to the rise in type 2 diabetes. <sup>13,15</sup> Notably, type 2 diabetes is more likely to occur in people with a higher BMI. 16 Additionally, as diabetes is more prevalent in older persons, aging is a contributing factor. 17 According to certain estimates, the majority of diabetic people globally (77.6%) would reside in developing countries by 2030.<sup>18</sup> From 1.8% of global GDP in 2015, the expense of disease management will rise to a maximum of 2.2%. <sup>19</sup> In this regard, blocking the enzymes that break down carbohydrates is regarded as a treatment option for type 2 diabetes. <sup>20</sup> The digesting enzyme  $\alpha$ -amylase is mostly released by the salivary glands and pancreas, with trace amounts found in other organs. One of the first enzymes to be studied scientifically was  $\alpha$ -amylase, which was first characterised in the early 1800s. This enzyme was dubbed " α-amylase" in the early 20th century, despite its original name being diastaste. Alpha-1,4glucan-4-glucanohydrolase, often known as  $\alpha$ -amylase, is an enzyme that acts on starch to randomly separate alpha-1,4-glucosidic bonds. It has a molecular weight of about 50,000, an optimal pH of 6.9, and requires chlorine for optimal action. Alpha amylases are found in the pancreas and saliva, whereas beta amylases (alpha-1,4-glucan-maltohydrolase) are found in plants.<sup>20</sup> Recent research suggests that a nonxanthine benzylidene indanone derivatives 2-(3,4-dihydroxybenzylidene)-4-methoxy-2,3-dihydro-1Hinden-1-one (2-BI), has shown to exhibit higher affinity at  $A_1/A_{2A}$  Ars compared to caffeine, and the structural similarity to caffeine which in turn established antidiabetic effect.<sup>14</sup>

A molecular framework containing 2-benzylidene-1-indanone derivatives from 1-indanone (1) and substituted benzaldehyde was created with the hope of demonstrating strong antidiabetic action in response to the parameters listed above, which prompted interest in carrying out this experiment. Moreover, ADME parameter analysis,  $\alpha$ -amylase (2QV4) docking investigations, spectrum characterisation, and in silico molecular docking were performed. Additionally, to find relationships between the chemical structure (or structurally related qualities) and the biological activity (or target property) of the synthesized compounds, structure-activity relationship (SAR) investigations were carried out.

# 2. Experimental

#### 2.1. Chemical Material and Apparatus

The reagents and chemicals employed were of the greatest quality, unless otherwise noted. They were used without additional purification after being acquired from Sigma-Aldrich Co., Acros Organics,

and Merck Chemical Co. Weighing was done using an analytical electronic balance. Merck silica gel was used for column chromatography (0.040-0.063 mm). A TLC aluminium sheet precoated with silica gel (silica gel  $60_{F254}$ ) was utilized for thin-layer chromatography, and it was visible under a UV lamp ( $\lambda_{max}$  = 254 nm and/or 366 nm). Chemical shifts were compared to dimethylsulfoxide-d<sub>6</sub> (2.50 ppm for <sup>1</sup>H NMR and 39.51 ppm for <sup>13</sup>C NMR) or chloroform-d<sub>1</sub> (7.24 ppm for <sup>1</sup>H NMR and 77.23 ppm for <sup>13</sup>C NMR). All NMR data were obtained using a Bruker Advance spectrometer (500 MHz for <sup>1</sup>H NMR and 125 MHz for <sup>13</sup>C NMR, Bruker Bioscience, Billerica, MA, USA). Perkin Elmer FT-IR spectroscopy (Perkin Elmer, Waltham, MA, USA) was used to record Fourier Transform Infrared (FT-IR) spectra using the ATR method in the frequency range of 4000 to 400 cm<sup>-1</sup>. A Waters Xevo QTOF MS (Milford, MA, USA) was used to record the mass spectra (HRMS). An open capillary tube was used to measure melting points at temperatures between 25 and 350°C using a Stuart Scientific SMP10 melting point apparatus (Staffordshire, UK).

## 2.2. Chemistry

#### 2.2.1. General Procedure for the Synthesis of 2-Benzylidene-1-Indanone Derivatives (3a-3p)

A mixture of 1-indanone 1 (6 mmol) and substituted benzaldehyde 2a-2p (6 mmol) in ethanol (15 mL) and the mixture was cooled to 5°C. Added 5% NaOH solution (15 mL) drop by drop over a period of 15 minutes after NaOH addition the ice bath was removed. The reaction mixture was stirred at room temperature for 10-12 hours; the reaction was monitored by TLC. After completion of the reaction, the reaction mixture was cooled to 5°C and stirred for 30 minutes at the same temperature. The mixture was recrystallized, filtered and the solid residue was washed with prechilled methanol. Dried the material under vacuum at 50°C gave the desired product 3a-3p (See Supporting Information Figures S1-S64).

- 2.2.1a. Synthesis of 2-(2-hydroxybenzylidene)-2,3-dihydro-1H-inden-1-one (3a): The procedure described in section 2.2.1 was employed with 1-indanone (1, 529 mg, 4 mmol) and 2-hydroxybenzaldehyde (2a, 488 mg, 4 mmol) in ethanol (10 mL), and 5% aqueous NaOH (10 mL) to yield 0.62 g (65.1%). Greenish yellow solid, m.p. 202-203°C;  $R_f \approx 0.25$  [UV-active, 30% EtOAc in *n*-Hexane]. IR  $v_{max}$ : 3390 (OH stretching), 3050 (=C-H stretching), 2895 (C-H stretching), 1654 (C=O), 1559 (C=C), 1435 (C=C), 1240 (C-O), 1135, 949, 734. ¹H NMR (500 MHz, DMSO-d<sub>6</sub>) δ ppm: 10.25 (s, O-H, 1H), 7.95 (s, H-10, 1H), 7.79 (d, J = 7.85 Hz, H-7, 1H), 7.74 (td, J = 7.85, 1.15 Hz, H-5, 1H), 7.70 (d, J = 7.00, H-6', 1H), 7.68 (d, J = 7.85 Hz, H-4, 1H), 7.48 (t, J = 7.85 Hz, H-6, 1H), 7.30 (t, J = 7.05 Hz, H-4', 1H), 6.97 (t, J = 7.00 Hz, H-5', 1H), 6.93 (d, J = 7.05 Hz, H-3', 1H), 4.08 (s, H-3, 2H).  $^{13}$ C NMR (125 MHz, DMSO-d<sub>6</sub>) δ ppm: 193.9 (C-1), 158.1 (C-2'), 150.5 (C-9), 137.9 (C-10), 135.1 (C-8), 133.9 (C-5), 131.9 (C-2), 130.0 (C-4'), 128.1 (C-6'), 128.0 (C-7), 127.1 (C-6), 123.9 (C-4), 122.2 (C-5'), 119.9 (C-3'), 116.4 (C-1'), 32.3 (C-3). HRMS (TOF-ES+): m/z 259.0735 ([M+Na]+ C<sub>16</sub>H<sub>12</sub>NaO<sub>2</sub>+ has theoritical value 259.0738).
- 2.2.1b. Synthesis of 2-(3-hydroxybenzylidene)-2,3-dihydro-1H-inden-1-one (3b): The procedure described in section 2.2.1 was employed with 1-indanone (1, 529 mg, 4 mmol) and 3-hydroxybenzaldehyde (2b, 488 mg, 4 mmol) in ethanol (10 mL), and 5% aqueous NaOH (10 mL) to yield 0.52 g (54.7%). Crimson white solid, m.p. 234-235 °C;  $R_f \approx 0.40$  [UV-active, 30% EtOAc in *n*-Hexane]. IR  $v_{max}$ : 3340 (OH stretching), 3044 (=C-H stretching), 2919 (Csp³-H), 1680 (C=O), 1614 (C=C), 1585 (C=C), 1439, 1255 (C-O), 1114, 740. ¹H NMR (500 MHz, DMSO-d<sub>6</sub>) δ ppm: 9.70 (s, O-H, 1H), 7.80 (d, J = 7.60 Hz, H-7, 1H), 7.74 (t, J = 7.50 Hz, H-5, 1H), 7.69 (d, J = 7.50 Hz, H-4, 1H), 7.49 (t, J = 7.60 Hz, H-6, 1H), 7.45 (s, H-10, 1H), 7.33 (t, J = 7.50 Hz, H-5′, 1H), 7.23 (d, J = 7.50 Hz, H-6′ 1H), 7.19 (s, H-2′, 1H), 6.89-6.87 (dd, J = 7.80, 1.65 Hz, H-4′, 1H), 4.10 (s, H-3, 2H). ¹³C NMR (125 MHz, DMSO-d<sub>6</sub>) δ ppm: 193.8 (C-1), 158.1 (C-3′), 150.4 (C-9′), 137.6 (C-10), 136.5 (C-8), 135.38 (C-1′), 135.32 (C-5), 133.5 (C-2), 130.4 (C-5′), 128.1 (C-7), 127.2 (C-6), 124.0 (C-4), 122.5 (C-6′), 117.5 (C-4′), 117.4 (C-2′), 32.4 (C-3). HRMS (TOF-ES+′): m/z 259.0735 ([M+Na]+ C<sub>16</sub>H<sub>12</sub>NaO<sub>2</sub>+ has theoritical value 259.0735).

- 2.2.1c. Synthesis of 2-(4-hydroxybenzylidene)-2,3-dihydro-1H-inden-1-one (3c): The procedure described in section 2.2.1 was employed with 1-indanone (1, 529 mg, 4 mmol) and 4-hydroxybenzaldehyde (2c, 488 mg, 4 mmol) in ethanol (10 mL), and 5% aqueous NaOH (10 mL) to yield 0.41 g (42.8%). Light greenish solid, m.p. 233-234°C;  $R_f \approx 0.3$  [UV-active, 30% EtOAc in *n*-Hexane]. IR  $v_{max}$ : 3309 (O-H), 3160 (=C-H), 1680 (C=O), 1504 (C=C), 1565 (C=C), 1270, 1164, 825, 729, 530. <sup>1</sup>H NMR (500 MHz, DMSO-d<sub>6</sub>) δ ppm: 10.15 (s, O-H, 1H), 7.77 (d, J = 7.50 Hz, H-7, 1H), 7.71 (t, J = 7.50 Hz, H-5, 1H), 7.67 (s, H-10, 1H), 7.65 (d, J = 8.50 Hz, H-2',6', 2H), 7.48 (d, J = 7.50 Hz, H-4, 1H), 7.46 (t, J = 7.50 Hz, H-6, 1H), 6.91 (d, J = 8.50 Hz, H-3', H-5', 2H), 4.06 (s, H-3, 2H). <sup>13</sup>C NMR (125 MHz, DMSO-d<sub>6</sub>) δ ppm: 193.7 (C-1), 159.8 (C-4'), 150.2 (C-9), 138.0 (C-10), 134.9 (C-8), 133.8 (C-5), 133.4 (C-2', C-6', 2C), 132.0 (C-2), 128.0 (C-1'), 127.0 (C-7), 126.4 (C-6), 123.8 (C-4), 116.5 (C-3', C-5', 2C), 32.4 (C-3). HRMS (TOF-ES<sup>+</sup>): m/z 259.0726 ([M+Na]<sup>+</sup> C<sub>16</sub>H<sub>12</sub>NaO<sub>2</sub><sup>+</sup> has theoritical value 259.0735).
- 2.2.1d. Synthesis of 2-(2-chlorobenzylidene)-2,3-dihydro-1H-inden-1-one (3d): The procedure described in section 2.2.1 was employed with 1-indanone (1, 661 mg, 5 mmol) and 2-chlorobenzaldehyde (2d, 703 mg, 5 mmol) in ethanol (13.5 mL), and 5% aqueous NaOH (13.5 mL) to yield 1.26 g (98.9%). Half-white solid, m.p. 153-154°C;  $R_f \approx 0.60$  [UV-active, 10% EtOAc in *n*-Hexane]. IR  $v_{max}$ : 3060 (=C-H stretching), 2360, 1695 (C=O), 1614 (C=C), 1265, 1085, 734 (=C-H), 665 (C-Cl). <sup>1</sup>H NMR (500 MHz, CDCl<sub>3</sub>) δ ppm: 8.06 (s, H=10, 1H), 7.94 (d, J = 8.00 Hz, H=7, 1H), 7.73 (d, J = 7.50 Hz, H=4, 1H), 7.63 (t, J = 7.50 Hz, H=5, 1H), 7.54 (d, J = 7.50 Hz, H=6', 1H), 7.49 (dd, J = 7.50, 1.30 Hz, H=3', 1H), 7.44 (t, J = 7.50 Hz, H=6, 1H), 7.38 (t, J = 7.5 Hz, H=4', 1H), 7.33 (t, J = 7.5 Hz, H=5', 1H), 3.98 (s, H=3, 2H). <sup>13</sup>C NMR (125 MHz, DMSO-d<sub>6</sub>) δ ppm: 193.0 (C=1), 150.2 (C=9), 137.6 (C=10), 136.9 (C=8), 135.2 (C=5), 134.9 (C=2'), 132.4 (C=1'), 131.1 (C=2), 130.4 (C=3'), 130.0 (C=4'), 127.8 (C=6'), 127.7 (C=7), 127.6 (C=5'), 126.7 (C=6), 123.8 (C=4), 31.3 (C=3). HRMS (TOF-ES+): m/z 255.0557 ([M+H]+ C<sub>16</sub>H<sub>12</sub>ClO+ has theoritical value 255.0576).
- 2.2.1e. Synthesis of 2-(4-chlorobenzylidene)-2,3-dihydro-1H-inden-1-one (3e): The procedure described in section 2.2.1 was employed with 1-indanone (1, 661 mg, 5 mmol) and 4-chlorobenzaldehyde (2e, 703 mg, 5 mmol) in ethanol (13.5 mL), and 5% aqueous NaOH (13.5 mL) to yield 1.25 g (98.1%). White solid, m.p. 179-181°C;  $R_f \approx 0.70$  [UV-active, 10% EtOAc in *n*-Hexane]. IR  $v_{max}$ : 3070 (=C-H stretching), 2950 (Csp³-H), 1690 (C=O stretching), 1604 (C=C stretching), 1265 (C-O stretching), 1085, 945, 820, 740, 509. ¹H NMR (500 MHz, CDCl₃) δ ppm: 7.91 (d, J = 7.50 Hz, H-7, 1H), 7.63 (t, J = 7.50 Hz, H-5, 1H), 7.63 (d, J = 8.5 Hz, H-2',6', 2H), 7.58 (s, H-10, 1H), 7.56 (d, J = 7.5 Hz, H-4, 1H), 7.44 (t, J = 7.50 Hz, H-6, 1H), 7.31 (d, J = 8.5 Hz, H-3', 5', 2H), 4.01 (s, H-3, 1H). ¹³C NMR (125 MHz, CDCl₃) δ ppm: 194.1 (C-1), 149.3 (C-9), 137.8 (C-10), 135.6 (C-8), 135.1 (C-5), 134.7 (C-4'), 133.8 (C-1'), 132.4 (C-2), 131.7 (C-1', C-6', 2C), 129.1 (C-3', C-5', 2C), 127.7 (C-7), 126.1 (C-6), 124.4 (C-4), 32.3 (C-3). HRMS (TOF-ES+): m/z 255.0555 ([M+H]+  $C_{16}H_{12}ClO^+$  has theoritical value 255.0576).
- 2.2.1 *f.* Synthesis of 2-(2,4-dichlorobenzylidene)-2,3-dihydro-1H-inden-1-one (3f): The procedure described in section 2.2.1 was employed with 1-indanone (1, 661 mg, 5 mmol) and 2,4-dichlorobenzaldehyde (2f, 875 mg, 5 mmol) in ethanol (13.5 mL), and 5% aqueous NaOH (13.5 mL) to yield 1.37 g (94.5%). White solid, m.p. 208-210°C;  $R_f \approx 0.70$  [UV-active, 10% EtOAc in *n*-Hexane]. IR  $v_{max}$ : 3055 (=C-H), 2919 (Csp³-H), 1690 (C=O), 1620 (C=C), 1465, 1105, 850, 740, 555. ¹H NMR (500 MHz, CDCl₃) δ ppm: 7.98 (s, H-10, 1H), 7.95 (d, J = 7.00 Hz, H-7, 1H), 7.67 (d, J = 7.5 Hz, H-6′, 1H), 7.65 (t, J = 7.00 Hz, H-5, 1H), 7.56 (d, J = 7.00 Hz, H-4, 1H), 7.52 (s, H-3′, 1H), 7.46 (t, J = 7.00 Hz, H-6, 1H), 7.37 (d, J = 7.50 Hz, H-5′, 1H), 3.98 (s, H-3, 2H). ¹³C NMR (125 MHz, CDCl₃) δ ppm: 193.5 (C-1), 149.4 (C-9), 137.8 (C-10), 137.3 (C-2′), 136.9 (C-8), 135.6 (C-5), 134.9 (C-2), 132.1 (C-1′), 130.4 (C-6′), 130.1 (C-3′), 128.6 (C-7), 127.8 (C-5′), 127.2 (C-6), 126.1 (C-4), 124.6 (C-4′), 31.8 (C-3). HRMS (TOF-ES⁺): m/z 286.1429 ([M+Na]+ C<sub>16</sub>H<sub>12</sub>O<sub>2</sub>Na+ has theoritical value 286.0739).
- 2.2.1g. Synthesis of 2-(4-fluorobenzylidene)-2,3-dihydro-1H-inden-1-one (3g): The procedure described in section 2.2.1 was employed with 1-indanone (1, 529 mg, 4 mmol) and 4-flurobenzaldehyde (2g, 496 mg, 4 mmol) in ethanol (10 mL), and 5% aqueous NaOH (10 mL) to yield 0.83 g (87.2%). White solid, m.p. 154-155°C;  $R_f \approx 0.50$  [UV-active, 10% EtOAc in *n*-Hexane]. IR  $\nu_{max}$ : 3055 (=C-H), 2360, 1664 (C=O), 1590 (C=C), 1499 (C=C), 1219 (C-F stretching), 1150, 835 (C-H bend), 725 (=C-H bending). <sup>1</sup>H

- NMR (500 MHz, CDCl<sub>3</sub>)  $\delta$  ppm: 7.93 (d, J = 8.00 Hz, H–7, 1H), 7.69-7.69 (s, H–10, 1H), 7.67 (d, J = 7.50 Hz, H–2′, H–6′, 2H), (d, J = 7.50 Hz, H–5, 1H), 7.58 (d, J = 7.50 Hz, H–4, 1H), 7.46 (t, J = 7.50 Hz, H–6, 1H), 7.16 (d, J = 7.50 Hz, H–3′, H–5′, 2H), 4.0 (s, H–3, 3H). <sup>13</sup>C NMR (125 MHz, CDCl<sub>3</sub>)  $\delta$  ppm: 194.2 (C–1), 164.3 (C–4′), 149.4 (C–9), 137.9 (C–10), 134.7 (C–8), 132.68 (C–5), 132.65 (C–2), 132.5 (C–7), 131.67 (C–2′), 131.64 (C–6′), 127.7 (C–1′), 126.1 (C–6), 124.4 (C–4), 116.2 (C–3′), 116.0 (C–5′), 32.3 (C–3). HRMS (TOF-ES<sup>+</sup>): m/z 239.0965 ([M+H]<sup>+</sup> C<sub>16</sub>H<sub>12</sub>FO<sup>+</sup> has theoritical value 239.0872).
- 2.2.1h. Synthesis of 2-(4-methoxybenzylidene)-2,3-dihydro-1H-inden-1-one (3h): The procedure described in section 2.2.1 was employed with 1-indanone (1, 397 mg, 3 mmol) and 4-methoxybenzaldehyde (2h, 409 mg, 3 mmol) in ethanol (8 mL), and 5% aqueous NaOH (8 mL) to yield 0.74 g (98.8%). Crimson white solid, m.p. 141-142°C;  $R_f \approx 0.20$  [UV-active, 10% EtOAc in *n*-Hexane]. IR  $v_{\text{max}}$ : 3079 (=C-H), 2925 (Csp³-H), 2840 (Csp³-H), 1685 (C=O), 1510 (C=C), 1510 (C=C), 1250 (C-O), 1020, 729, 520. ¹H NMR (500 MHz, CDCl₃) δ ppm: 7.90 (d, J = 7.50 Hz, H-7, 1H), 7.63-7.63 (d, J = 8.5 Hz, H-2', H-6', 2H), 7.63 (t, J = 7.50 Hz, H-5, 1H), 7.59 (d, J = 7.50 Hz, H-4, 1H), 7.54 (s, H-10, 1H), 7.41 (t, J = 7.50 Hz, H-6, 1H), 6.98 (d, J = 8.50 Hz, H-3', H-5', 2H), 3.99 (s, H-3, 2H), 3.85 (s, H-7', 3H). ¹³C NMR (125 MHz, CDCl₃) δ ppm: 194.4 (C-1), 160.8 (C-4'), 149.5 (C-9), 138.2 (C-10), 134.3 (C-8), 133.8 (C-5), 132.5 (C-2), 132.4 (C-2', C-6', 2C), 128.1 (C-1'), 127.5 (C-7), 126.1 (C-6), 124.3 (C-4), 114.4 (C-3', C-5', 2C), 66.4 (C-7'), 32.4 (C-3). HRMS (TOF-ES+): m/z 251.1068 ([M+H]+ C<sub>17</sub>H<sub>15</sub>O<sub>2</sub>+ has theoritical value 251.1072).
- 2.2.1i. Synthesis of 2-(4-bromobenzylidene)-2,3-dihydro-1H-inden-1-one (3i): The procedure described in section 2.2.1 was employed with 1-indanone (1, 397 mg, 3 mmol) and 4-bromobenzaldehyde (2i, 555 mg, 3 mmol) in ethanol (8 mL), and 5% aqueous NaOH (8 mL) to yield 0.69 g (76.2%). White solid, m.p. 185-186°C;  $R_f \approx 0.50$  [UV-active, 10% EtOAc in *n*-Hexane]. IR  $v_{max}$ : 3055 (=C-H), 2924 (Csp³-H), 1690 (C=O), 1614 (C=C), 1405, 1265, 1064, 815, 729, 509. ¹H NMR (500 MHz, CDCl₃)  $\delta$  ppm: 7.91 (d, J = 8.00 Hz, H-7, 1H), 7.64 (t, J = 8.00 Hz, H-5, 1H), 7.59 (d, J = 7.5 Hz, H-2′, H-6′, 2H), 7.57 (d, J = 7.5 Hz, H-3′, H-5′, 2H), 7.53 (s, H-10, 1H), 7.51 (d, J = 8.00 Hz, H-4, 1H), 7.43 (t, J = 8.00 Hz, H-6, 1H), 4.00 (s, H-3, 2H). ¹³C NMR (125 MHz, CDCl₃)  $\delta$  ppm: 194.1 (C-1), 149.4 (C-9), 137.8 (C-10), 135.3 (C-8), 134.8 (C-5), 134.2 (C-1′), 132.5 (C-2), 132.2 (C-3′, C-5′, 2C), 132.0 (C-2′, C-6′, 2C), 127.8 (C-7), 126.2 (C-6), 124.5 (C-4), 124.0 (C-4′), 32.3 (C-3). HRMS (TOF-ES+): m/z 286.1429 ([M+Na]+  $C_{16}H_{12}O_2Na^+$  has theoritical value 286.0739).
- 2.2.1j. Synthesis of 2-(3,5-dimethoxybenzylidene)-2,3-dihydro-1H-inden-1-one (3j): The procedure described in section 2.2.1 was employed with 1-indanone (1, 397 mg, 3 mmol) and 3,5-dimethoxybenzaldehyde (2j, 499 mg, 3 mmol) in ethanol (8 mL), and 5% aqueous NaOH (8 mL) to yield 0.79 g (93.2%). White solid, m.p. 174-175°C;  $R_f \approx 0.30$  [UV-active, 10% EtOAc in n-Hexane]. IR  $v_{max}$ : 3015 (=C-H), 2924 (Assym. Csp³-H), 1685 (C=O), 1575 (C=C), 1444 (C=C), 1185 (C-O), 1054, 988, 725. ¹H NMR (500 MHz, CDCl₃)  $\delta$  ppm: 7.91 (d, J = 7.50 Hz, H-7, 1H), 7.62-7.58 (m, H-4, H-5, 2H), 7.55 (s, H-10, 1H), 7.42 (t, J = 7.50 Hz, H-6, 1H), 6.81 (s, H-2',6', 2H), 6.51 (s, H-4', 1H), 4.03 (s, H-3, 2H), 3.84 (s, H-7', H-8', 6H). ¹³C NMR (125 MHz, CDCl₃)  $\delta$  ppm: 194.3 (C-1), 160.9 (C-3', C-5', 2C), 149.6 (C-9), 137.9 (C-10), 137.1 (C-8), 135.1 (C-5), 134.7 (C-2), 133.9 (C-1'), 127.7 (C-7), 126.1 (C-6), 124.4 (C-4), 108.7 (C-2', C-6', 2C), 101.7 (C-4'), 55.4 (C-7', C-8', 2C), 32.3 (C-3). HRMS (TOF-ES+): m/z 281.1178 ([M+H]+  $C_{18}H_{17}O_3^+$  has theoritical value 281.1177).
- 2.2.1k. Synthesis of 2-(2,4-dimethoxybenzylidene)-2,3-dihydro-1H-inden-1-one (3k): The procedure described in section 2.2.1 was employed with 1-indanone (1, 397 mg, 3 mmol) and 2,4-dimethoxybenzaldehyde (2k, 499 mg, 3 mmol) in ethanol (8 mL), and 5% aqueous NaOH (8 mL) to yield 0.68 g (80.2%). Greenish yellow solid, m.p. 127-128°C;  $R_f \approx 0.20$  [UV-active, 10% EtOAc in *n*-Hexane]. IR  $v_{max}$ : 2934 (Csp³-H), 2835 (sym. Csp³-H), 1685 (C=O), 1595 (C=C), 1455 (C=C), 1255 (C-O), 1085, 825, 729. ¹H NMR (500 MHz, CDCl₃) δ ppm: 8.12 (s, H=10, 1H), 7.91 (d, J = 7.50 Hz, H=6′, 1H), 7.66 (d, J = 7.50 Hz, H=7, 1H), 7.58 (t, J = 7.50 Hz, H=5, 1H), 7.53 (d, J = 7.55 Hz, H=4, 1H), 7.41 (t, J = 7.50 Hz, H=6, 1H), 6.58 (d, J = 7.50 Hz, H=5′, 1H), 6.48 (s, H=3′, 1H), 3.95 (s, H=3, 2H), 3.88 (s, H=7′, 3H), 3.86 (s, H=8′, 3H). ¹³C NMR (125 MHz, CDCl₃) δ ppm: 194.4 (C=1), 162.5 (C=4′), 160.7 (C=9), 149.5 (C=2′), 138.4 (C=10), 134.0 (C=8), 132.1 (C=5), 130.8 (C=2), 128.2 (C=6′), 127.4 (C=7), 126.0

- (C-6), 124.2 (C-4), 117.5 (C-1'), 105.2 (C-5'), 98.2 (C-3'), 55.6 (C-7'), 55.4 (C-8'), 32.5 (C-3). HRMS (TOF-ES<sup>+</sup>): m/z 281.1174 ([M+H]<sup>+</sup> C<sub>18</sub>H<sub>17</sub>O<sub>3</sub><sup>+</sup> has theoritical value 281.1177).
- 2.2.11. Synthesis of 2-(3,4,5-trimethoxybenzylidene)-2,3-dihydro-1H-inden-1-one (31): The procedure described in section 2.2.1 was employed with 1-indanone (1, 397 mg, 3 mmol) and 3,4,5-trimethoxybenzaldehyde (21, 589 mg, 3 mmol) in ethanol (8 mL), and 5% aqueous NaOH (8 mL) to yield 0.81 g (86.5%). Crimson yellow solid, m.p.  $163-164^{\circ}$ C;  $R_f \approx 0.20$  [UV-active, 10% EtOAc in n-Hexane]. IR  $v_{max}$ : 2929 (Csp³-H), 2835 (Csp³-H), 1685 (C=O), 1575 (C=C), 1455 (C=C), 1255, 1125, 1130 (C-O), 995, 729. ¹H NMR (500 MHz, CDCl₃)  $\delta$  ppm: 7.94 (d, J = 7.50 Hz, H-7, 1H), 7.64 (d, J = 7.50 Hz, H-5, 1H), 7.61 (s, H-10, 1H), 7.60 (d, J = 7.5 Hz, H-4, 1H), 7.45 (t, J = 7.50 Hz, H-6, 1H), 6.93 (s, H-2', H-6', 2H), 4.06 (s, H-3, 2H), 3.96 (s, H-7', H-9', 6H), 3.93 (s, H-8', 3H). ¹³C NMR (125 MHz, CDCl₃)  $\delta$  ppm: 194.2 (C-1), 153.3 (C-3', C-5', 2C), 149.3 (C-9), 139.7 (C-10), 138.0 (C-4'), 134.6 (C-8), 134.1 (C-5), 133.7 (C-2), 130.9 (C-7), 127.7 (C-6), 126.1 (C-4), 124.4 (C-1'), 108.1 (C-2', C-6', 2C), 61.0 (C-8'), 56.2 (C-7', C-9', 2C), 32.2 (C-3). HRMS (TOF-ES+): m/z 311.1287 ([M+H]+ C<sub>19</sub>H<sub>19</sub>O<sub>4</sub>+ has theoritical value 311.1283).
- 2.2.1*m*. Synthesis of 2-(Naphthalylbenzylidene)-2,3-dihydro-1H-inden-1-one (3*m*): The procedure described in section 2.2.1 was employed with 1-indanone (1, 925 mg, 7 mmol) and 1-Naphthaldehyde (2*m*, 1093 mg, 7 mmol) in ethanol (17.5 mL), and 5% aqueous NaOH (17.5 mL) to yield 1.53 g (81.1%). Light yellowish solid, m.p. 126-127°C;  $R_f \approx 0.60$  [UV-active, 10% EtOAc in *n*-Hexane]. IR  $v_{max}$ : 3050 (=C-H), 1685 (C=O), 1609 (C=C), 1329, 1090, 945, 729. ¹H NMR (500 MHz, CDCl<sub>3</sub>) δ ppm: 8.48 (s, H–10, 1H), 8.26 (d, J = 8.00 Hz, H–8′, 1H), 7.99 (d, J = 8.00 Hz, H–2′, 1H), 7.93 (d, J = 8.00 Hz, H–4′, H–5′, 2H), 7.82 (d, J = 7.00 Hz, H–7, 1H), 7.65 (d, J = 7.50 Hz, H–4, 1H), 7.62 (d, J = 7.50 Hz, H–5, 1H), 7.59 (t, J = 8.00 Hz, H–3′, 1H), 7.57 (t, J = 8.00 Hz, H–7′, 1H), 7.54 (t, J = 8.00 Hz, H–6′, 1H), 7.46 (t, J = 7.00 Hz, H–6, 1H), 4.01 (s, H–3, 2H).  $^{13}$ C NMR (125 MHz, CDCl<sub>3</sub>) δ ppm: 194.0 (C–1), 150.0 (C–9), 138.2 (C–10), 137.1 (C–1′), 134.7 (C–8), 133.6 (C–5), 132.3 (C–10′), 130.9 (C–2), 129.9 (C–5′), 128.7 (C–4′), 127.6 (C–7, C–7′, 2C), 127.0 (C–9′), 126.8 (C–3′), 126.3 (C–6), 126.2 (C–6′), 125.2 (C–4), 124.5 (C–8′), 124.0 (C–2′), 32.0 (C–3). HRMS (TOF-ES+′): m/z 271.1124 ([M+H]+ C<sub>20</sub>H<sub>15</sub>O+′ has theoritical value 271.1122).
- 2.2.1n. Synthesis of 2-(3-nitrobenzylidene)-2,3-dihydro-1H-inden-1-one (3n): The procedure described in section 2.2.1 was employed with 1-indanone (1, 793 mg, 6 mmol) and 3-nitrobenzaldehyde (2n, 907 mg, 6 mmol) in ethanol (15 mL), and 5% aqueous NaOH (15 mL) to yield 1.44 g (90.3%). Light yellowish solid, m.p. 199-200°C;  $R_f \approx 0.80$  [UV-active, 10% EtOAc in n-Hexane]. IR  $v_{max}$ : 3074 (=C-H), 2859 (Csp<sup>3</sup>-H), 1685 (C=O), 1520 (NO<sub>2</sub>), 1284, 1085, 734, 655, 555. <sup>1</sup>H NMR (500 MHz, CDCl<sub>3</sub>) δ ppm: 8.53 (s, H-2', 1H), 8.25 (dd, J = 8.50 Hz, H-4', 1H), 7.92 (t, J = 8.50 Hz, H-5', H-6', 2H), 7.68 (s, H-10, 1H), 7.66 (d, J = 8.00 Hz, H-7, 1H), 7.64 (d, J = 8.00 Hz, H-5, 1H), 7.61 (d, J = 8.00 Hz, H-4, 1H), 7.45 (t, J = 8.00 Hz, H-6, 1H), 4.11 (s, H-3, 2H). <sup>13</sup>C NMR (125 MHz, CDCl<sub>3</sub>) δ ppm: 193.7 (C-1), 149.3 (C-3'), 148.6 (C-9), 137.5 (C-10), 137.4 (C-1'), 137.0 (C-8), 136.5 (C-6'), 135.2 (C-5), 130.8 (C-2), 130.0 (C-5'), 128.0 (C-7), 126.3 (C-6), 124.6 (C-4), 124.2 (C-4'), 123.9 (C-2'), 32.2 (C-3). HRMS (TOF-ES<sup>+</sup>): m/z 266.0816 ([M+H]<sup>+</sup> C<sub>16</sub>H<sub>12</sub>NO<sub>3</sub><sup>+</sup> has theoritical value 266.0817).
- 2.2.1o. Synthesis of 2-(4-isopropylbenzylidene)-2,3-dihydro-1H-inden-1-one (3o): The procedure described in section 2.2.1 was employed with 1-indanone (1, 793 mg, 6 mmol) and 4-isopropylbenzaldehyde (2o, 889 mg, 6 mmol) in Ethanol (15 mL), and 5% aqueous NaOH (15 mL) to yield 1.28 g (81.5%). Light brown solid, m.p. 78-79°C;  $R_f \approx 0.50$  [UV-active, 10% EtOAc in *n*-Hexane]. IR  $v_{\text{max}}$ : 3034 (=C-H), 2950 (Csp³-H), 2859 (sym. Csp³-H), 1690 (C=O), 1600 (C=C), 1460, 1265 (C-O), 1090, 825, 740, 550. ¹H NMR (500 MHz, CDCl₃) δ ppm: 7.92 (d, J = 7.50 Hz, H-7, 1H), 7.67 (s, H-10, 1H), 7.63 (d, J = 7.50 Hz, H-2′, H-6′, 2H), 7.61 (t, J = 7.50, H-5, 1H), 7.56 (d, J = 7.50, H-4, 1H),7.42 (t, J = 7.50 Hz, H-6, 1H), 7.33 (d, J = 8.50 Hz, H-3′, H-5′, 2H), 4.04 (s, H-3, 2H), 2.96 (m, H-1″, 1H), 1.29 (d, J = 6.90 Hz, H-2″, 6H),  $^{13}$ C NMR (125 MHz, CDCl₃) δ ppm: 194.5 (C-1′), 151.0 (C-4′), 149.6 (C-9), 138.1 (C-10), 134.5 (C-8), 134.0 (C-5), 133.8 (C-1′), 133.0 (C-2), 130.9 (C-2′, C-6′, 2C), 127.6 (C-7), 127.1 (C-6), 126.1 (C-3′, C-5′, 2C), 124.4 (C-4), 34.1 (C-1″), 32.5 (C-3), 23.8 (C-2″, 2C). HRMS (TOF-ES+): m/z 263.1436 ([M+H]+ C<sub>19</sub>H<sub>19</sub>O+ has theoritical value 263.1435).

2.2.1p. Synthesis of 2-(2-methoxybenzylidene)-2,3-dihydro-1H-inden-1-one (3p): The procedure described section 2.2.1 was employed with 1-indanone (1, 793 mg, 6 mmol) and 2-methoxybenzaldehyde (2p, 817 mg, 6 mmol) in ethanol (15 mL), and 5% aqueous NaOH (15 mL) to yield 1.39 g (92.7%). Light yellowish solid, m.p. 132-133°C;  $R_f \approx 0.80$  [UV-active, 10% EtOAc in *n*-Hexane]. IR  $v_{max}$ : 3039 (=C-H), 2950 (Csp³-H), 2895 (sym. Csp³-H), 1690 (C=O), 1620 (C=C), 1245 (C-O), 1080, 729, 550. ¹H NMR (500 MHz, CDCl₃) δ ppm: 8.14 (s, H=10, 1H), 7.91 (d, J = 7.50 Hz, H=7, 1H), 7.68 (d, J = 8.00 Hz, H=6′, 1H), 7.59 (t, J = 7.50 Hz, H=5, 1H), 7.53 (d, J = 7.50 Hz, H=4, 1H), 7.41 (d, J = 7.50 Hz, H=6, 1H), 7.37 (d, J = 8.50 Hz, H=4′, 1H), 7.02 (t, J = 8.00 Hz, H=5′, 1H), 6.95 (d, J = 8.50 Hz, H=3′, 1H), 3.99 (s, H=3, 2H), 3.89 (s, H=7′, 3H). ¹³C NMR (125 MHz, CDCl₃) δ ppm: 194.3 (C=1), 159.1 (C=2′), 149.7 (C=9), 138.2 (C=10), 134.6 (C=8), 134.4 (C=5), 131.1 (C=2), 129.6 (C=4′), 128.5 (C=6′), 127.5 (C=7), 126.1 (C=6), 124.44 (C=4), 124.40 (C=5′), 120.4 (C=1′), 111.0 (C=3′), 55.5 (C=7′), 32.3 (C=3). HRMS (TOF-ES¹): m/z 251.1069 ([M+H]† C<sub>17</sub>H<sub>15</sub>O<sub>2</sub>† has theoritical value 251.1072.

#### 2.3. Biological Assay

## 2.3.1 Inhibition of the $\alpha$ -Amylase Enzyme

In this test, the technique given by Abu Bakar et al. was followed with modest alterations. For the investigation, 3,5-dinitrosalicylic acid (DNSA), human pancreatic  $\alpha$ -amylase, and acarbose were acquired.<sup>21</sup> To make the  $\alpha$ -amylase solution, 0.025 g of the enzyme was dissolved in 50 mL of phosphate buffer (20 mM, pH 6.9). In 350 millilitres of distilled water, 5 grams of 3,5-dinitrosalicylic acid, 8 grams of sodium hydroxide, and 150 grams of sodium potassium tartrate were dissolved to prepare the colorimetric reagent. A magnetic stirrer was used to completely mix the mixture, and distilled water was added to get the final volume down to 500 mL. A 1% starch solution was made by boiling 0.25 g of starch in 50 mL of sodium acetate buffer (20 mM, pH 6.9) while stirring constantly for 15 minutes. <sup>21-23</sup> A stock solution containing 500 µg/mL of the samples was made. After weighing the sample (in the proper quantity), it was dissolved in 200 µL of chloroform in 1% DMSO (2.4 µg/mL). Following that, the resultant stock solution was diluted to various concentrations (15.6-250 µM). A sample of 100 µL was added to a tube containing 200 μL of α-amylase solution diluted and 100 μL starch in 20 mM sodium phosphate buffer (pH 6.9). After 10 minutes of incubation at 37 °C, 300 µL of dinitrosalicylic acid (DNS) reagent was added to stop the reaction. After 10 minutes in a boiling water bath, the tubes were taken out and allowed to cool to room temperature before being diluted with 300 µL of distilled water. The MPR-96 microplate reader (Halo, Dynamica, Australia) was used to measure the absorbance of the final product at 620 nm after 100 µL of the reaction mixture had been pipetted into a 96-well microplate. The same procedure was used to prepare the positive control, substituting the sample with the acarbose. <sup>21-23</sup> The inhibitory activity of  $\alpha$ -amylase was determined using the following formula. <sup>15</sup>:

$$Percentage\ inhibition\ (\%) = \frac{(Abs.\ control-Abs.\ sample)}{(Abs.\ control)} X\ 100$$

# 2.3.2. Statistical Analysis

All assays were conducted as three independent experiments; each performed in duplicate. The results are presented as mean  $\pm$  SD (n = 3). Statistical significance of the inhibitory effects of synthesized compounds compared with acarbose was determined by one-way ANOVA with p < 0.05 considered significant. Representative dose—response curves are provided in the Supplementary Information.

#### 2.4 Molecular Docking

The Protein Data Bank supplied the crystal structure of pancreatic  $\alpha$ -amylase (pdb id: 2QV4) complexed with nitrate and acarbose at 1.97 Å resolution (http://www.rcsb.org/pdb, retrieved on 15 November 2024). In AutoDock, the polar hydrogen atoms, Kollman charges, and Gasteiger charges were added after the water molecules were eliminated and the non-polar hydrogen atoms were combined.<sup>24</sup>

ChemDraw 16.0 was used to sketch the structure of ligands 3a-3p, which were then converted into SMILES format. The SMILES codes were subsequently imported into Chem 3D 21.0.0, where the 3D structures were generated, energy-minimized, and saved in .pdb format. To make the .pdb file compatible with AutoDock 1.5.6 tools, it was changed to .pdbqt format. The grid's size was 50 x 50 x 50 points with a 0.375 Å spacing, and it was centered at the crystallographic coordinates of nitrate (central x = 13.758; center y = 58.583; and center z = 22.465). The conformers with the lowest docking score were found using the Lamarckian Genetic Algorithm, and a .dpf file was created for docking. In order to better understand the remaining interactions of the most stable ligand-protein complexes produced, the compounds were progressively docked to human pancreatic α-amylase (PDB ID: 2QV4) in the final docking operation. To evaluate the ligand's binding interactions with the target across different conformations, the docked file was saved in dlg format and examined. After choosing the conformation with the highest docking score, Biovia Discovery Studio 2021 was used to visualize its interactions. <sup>22,23,25</sup> The ground state energy pose attained on re-docking and the co-crystallized ligands were superimposed, and its root mean square deviation (RMSD) score was calculated between these two superimposed ligands poses, <sup>26</sup> with a score of -8.2 Kcal/mol, the identical pose of co-crystallized ligand in the crystal structure (RMSD = 0.53 Å) was employed in accordance with a validation technique to replicate via docking.<sup>27,28</sup>

The three-dimensional structure of human pancreatic  $\alpha$ -amylase (PDB ID: 2QV4) was selected for docking studies. This structure has been experimentally determined using X-ray diffraction at a high resolution of 1.97 Å, ensuring reliable atomic positioning and accurate active site geometry. In this study, the stereochemical quality of the protein was validated through a Ramachandran plot generated using POCHECK (https://saves.mbi.ucla.edu/results?job=329492&p=procheck). The plot showed that 100% of residues are located within the most favoured and allowed regions (Figure S66). This conforms the high quality of the  $\alpha$ -amylase structure, making it suitable for molecular docking evaluations.

#### 2.5 Physicochemical, Drug Likeness and ADME Properties

The Swiss Prediction web tool was used to estimate the ADME characteristics and drug resemblance of 2-benzylidene-1-indanone derivatives **3a-3p**.<sup>29</sup> In order to forecast the physicochemical, ADME, and drug-likeness qualities, the structures of compounds **3a-3p** and acarbose were created in ChemDraw 16.0, duplicated as SMILES, and then uploaded one at a time to a web tool.<sup>22</sup>

### 3. Results and Discussion

# 3.1. Chemistry

Syntheses of sixteen substituted 2-benzylidene-1-indanone derivatives **3a–3p** was depicted in Scheme 1. Compound **3a-3p** were prepared by combining substituted benzaldehydes (**2a-2p**) with 1-indanone (**1**) in a protic solvent at room temperature with diluted NaOH via Aldol condensation in a yield of 42–98%. The FT-IR, <sup>1</sup>H, and <sup>13</sup>C NMR spectra of the synthesized compounds **3a-3p** verified the production of substituted 2-benzylidene-1-indanone derivatives. Aromatic =C-H stretching peaked at 3079-3015 cm<sup>-1</sup>, carbonyl C=O stretching caused absorptions at 1635-1654 cm<sup>-1</sup>, aromatic C=C stretching occurred at 1609-1555 cm<sup>-1</sup>, and alkyl C=C stretching occurred at 1455-1444 cm<sup>-1</sup>. Aromatic hydrogen signals range from 6.9 to 8.4 ppm in the <sup>1</sup>H NMR spectra. The compounds' <sup>13</sup>C NMR data revealed a distinctive C=O signal at 193–195 ppm. The methylene (CH<sub>2</sub>) carbons of the indanone moiety appeared as a distinctive peak at 32 ppm. Lastly, as shown in the supplementary file, the synthesised molecules [M+Na]<sup>+</sup> or [M+H]<sup>+</sup> ions were confirmed by HREIMS (TOF-ES<sup>+</sup>) data (see Supporting Information Figures S1-S64).

Selvakumar et al., Org. Commun. (20XX) XX:X XX-XX

O CHO
$$R^{1} = 5\% \text{ NaOH}$$
(2a-2p)
(3a-3p)

a:  $R^{1} = OH$ ,  $R_{2} = R_{3} = R_{4} = H$ 
b:  $R^{2} = OH$ ,  $R_{1} = R_{2} = R_{4} = H$ 
c:  $R^{3} = OH$ ,  $R_{1} = R_{2} = R_{4} = H$ 
d:  $R^{1} = Cl$ ,  $R^{2} = R_{3} = R^{4} = H$ 
e:  $R^{3} = Cl$ ,  $R_{1} = R^{2} = R^{4} = H$ 
f:  $R^{1} = R_{3} = Cl$ ,  $R_{2} = R_{4} = H$ 
g:  $R^{3} = F$ ,  $R^{1} = R_{2} = R_{4} = H$ 
h:  $R^{3} = OMe$ ,  $R_{1} = R_{2} = R_{4} = H$ 
g:  $R^{3} = F$ ,  $R^{1} = R_{2} = R_{4} = H$ 
h:  $R^{2} = OMe$ ,  $R^{1} = R_{2} = R_{4} = H$ 
g:  $R^{3} = F$ ,  $R^{1} = R_{2} = R_{4} = H$ 
p:  $R^{1} = OMe$ ,  $R^{2} = R_{3} = R_{4} = H$ 
p:  $R^{1} = OMe$ ,  $R^{2} = R_{3} = R_{4} = H$ 
p:  $R^{1} = OMe$ ,  $R^{2} = R_{3} = R_{4} = H$ 

Scheme 1. Synthetic pathway for the preparation of substituted 2-benzylidene-1-indanone derivatives

#### 3.2. In vitro α-Amylase Inhibitory Activity

The *in vitro*  $\alpha$ -amylase inhibitory activity of substituted 2-benzylidene-1-indanone derivatives (3a–3p) was assessed and compared with acarbose (Table 1). Compounds 3a, 3e, 3g, 3h, and 3j showed promising inhibition against  $\alpha$ -amylase with IC<sub>50</sub> values ranging from 17.3-19.8  $\mu$ M when compared to a positive control with an IC<sub>50</sub> value of  $21.3 \pm 3.5 \mu$ M, according to the *in vitro* inhibition of  $\alpha$ -amylase at various concentrations (15.6–250  $\mu$ M). This led to the conclusion that compounds 3a and 3e were the most promising. With the exception of compounds 3b and 3c, which had IC<sub>50</sub> values of 34.5  $\pm$  10.0 and 35.5  $\pm$  8.7  $\mu$ M, respectively, all other derivatives displayed modest activity in comparison to the positive control.

The current investigation was designed specifically as a preliminary enzymatic screening against pancreatic  $\alpha$ -amylase, which is a clinically validated target for modulating starch digestion and managing postprandial hyperglycaemia. The choice of  $\alpha$ -amylase inhibition as the sole assay was based on its well-established therapeutic relevance, exemplified by the clinically used inhibitor acarbose. While the observed ICso values demonstrated that several of our derivatives were more potent than acarbose, we acknowledge that diabetes is a multifactorial disease involving additional targets such as  $\alpha$ -glucosidase and glucose transport pathways. Future studies will therefore extend our evaluation to complementary assays, including  $\alpha$ -glucosidase inhibition and cellular glucose uptake, to provide a more comprehensive pharmacological profile.

Table 1. α-Amylase inhibition activity of substituted 2-benzylidene-1-indanone 3a-3p

Comounds	IC <sub>50</sub> (μM)	Comounds	$IC_{50} (\mu M)$
3a	$17.7 \pm 1.4$	3i	$25.3 \pm 1.0$
3b	$34.5 \pm 10.0$	3j	$19.7 \pm 1.2$
3c	$35.5 \pm 8.7$	3k	$28.2 \pm 1.6$
<b>3</b> d	$24.2 \pm 1.1$	31	$28.2 \pm 1.7$
<b>3</b> e	$17.3 \pm 1.7$	3m	$27.8 \pm 3.6$
<b>3</b> f	$26.1 \pm 1.8$	3n	$27.8 \pm 1.0$
3g	$19.0 \pm 4.6$	30	$30.0\pm2.5$
3h	$19.8 \pm 1.0$	<b>3</b> p	$22.4\pm2.3$
		Acarbose	$30.2\pm1.9$
		(control)	

Results are expressed as mean  $\pm$  SD (n=3) of at least three independent experiments.

#### 3.3. Molecular Docking Studies

To investigate their interactions, the docked compounds were evaluated for antidiabetic activity with human pancreatic  $\alpha$ -amylase (PDB ID: 2QV4) using AutoDock tools 1.5.6.<sup>22</sup> The substituted 2-benzylidene-1-indanone derivatives (**3a-3p**) of antidiabetic drugs were shown to target the pancreatic  $\alpha$ -amylase, which is crucial for the control of glucose and homeostasis. The chosen crystal structure (2QV4) provides a high-resolution (1.97 Å) model of human  $\alpha$ -amylase with acarbose, a clinically used inhibitor, <sup>30</sup> which allowed for accurate identification of active site residues and validation of the docking protocol by redocking the reference ligand. This ensured the reliability of subsequent docking evaluations with the synthesized 2-benzylidene-1-indanone derivatives. Moreover, evaluating binding interactions within this target enabled a deeper understanding of the structural basis for enzyme inhibition and supported the structure-activity relationship (SAR) findings from *in vitro* assays.<sup>30</sup>

Tables 2 and 3 list the amino acid residues of compounds 3a, 3e, 3g, 3h, and 3j along with their docking score. Additionally, as a reference, the typical medication acarbose was also put through the docking analysis. Following the molecular docking procedure, it was discovered that all five of the proposed analogues were active against the  $\alpha$ -amylase and had higher binding energies (varying from -8.2 to -9.8 kcal/mol) than acarbose. Tables 2 and 3 provide summaries of these compounds' docking interactions and docking score, respectively. Additionally, Figure 1(a-d) displays the 3D representations of 3a, 3e, 3g, 3h, and 3j together with their protein interactions (see also Supporting Information Figure S65).

**Table 2.** In silico binding energy between compounds with  $\alpha$ -amylase

Compounds	Docking score (kcal/mol)
3a	$-8.9 \pm 0.0$
<b>3</b> b	$-9.1 \pm 0.2$
3c	$-9.3 \pm 0.1$
<b>3</b> d	$-9.4\pm0.0$
<b>3e</b>	$-9.0 \pm 0.0$
<b>3</b> f	$-9.4 \pm 0.0$
<b>3</b> g	$-9.2 \pm 0.1$
3h	$-8.9 \pm 0.1$
3i	$-8.9 \pm 0.1$
3j	$-8.5 \pm 0.1$
3k	$-8.3 \pm 0.2$
31	$-8.2 \pm 0.2$
3m	$-9.8 \pm 0.0$
3n	$-9.2 \pm 0.0$
30	$-9.2 \pm 0.0$
<b>3</b> p	$-8.5 \pm 0.1$
Acarbose	$-7.8 \pm 0.0$

# Selvakumar et al., Org. Commun. (20XX) XX:X XX-XX

Results are expressed as mean  $\pm$  SD (n=3) of at least three independent experiments.

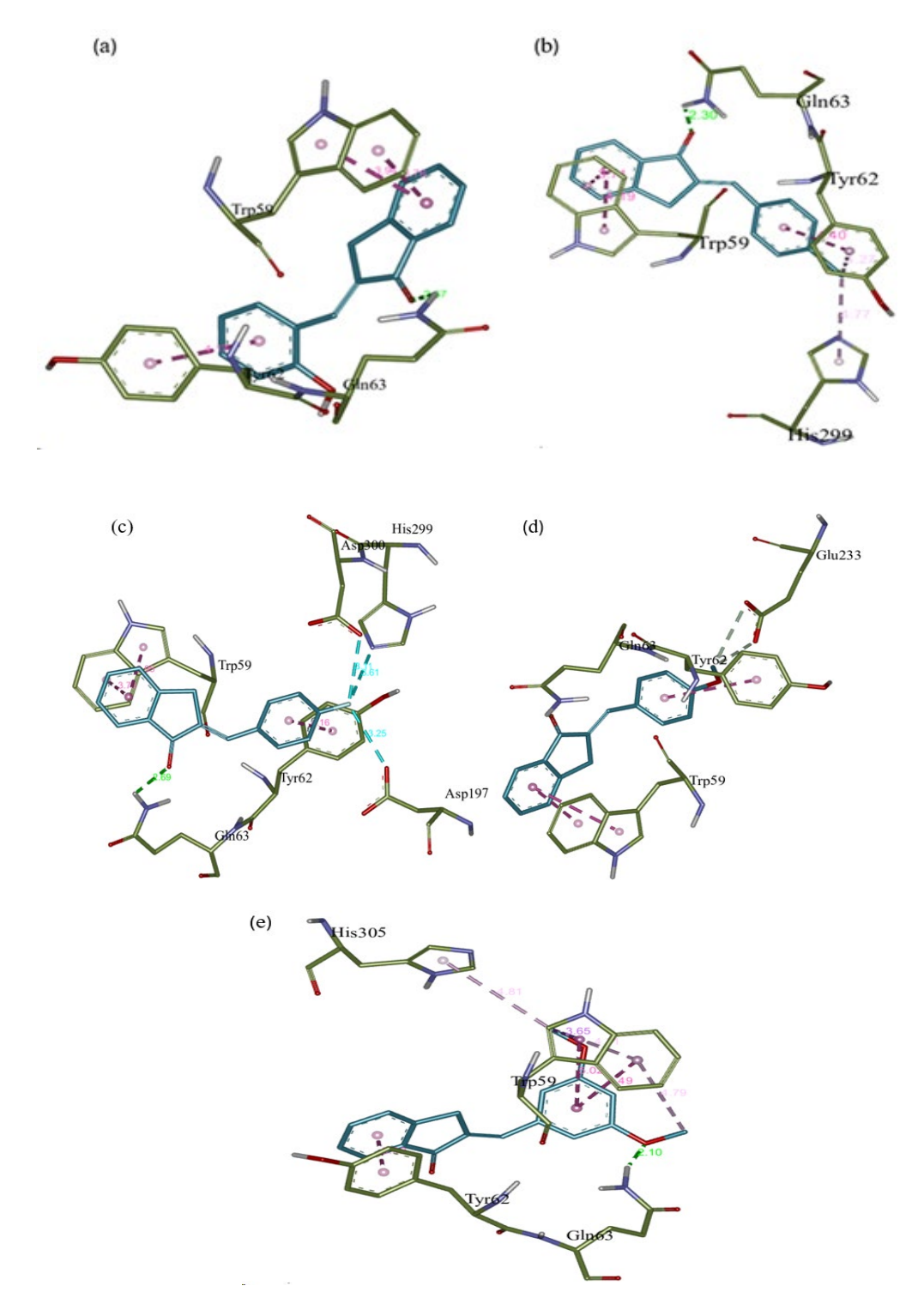


Figure 1. 3D representations of the binding modes of compounds 3a(a), 3e(b), 3g(c), 3h(d), 3j(e) to human pancreatic  $\alpha$ -amylase (PDB ID: 2QV4)

	-	-	• •
Compound	Moiety	Residue	Types of interaction
S			
3a	C=O	GLN63	Conventional H-bond (2.67 Å)
	Phenyl	TRP59	π- π Stacked
	Phenyl	TYR62	π- π Stacked
<b>3e</b>	-C=O	GLN63	Conventional H-bond (2.30 Å)
	Phenyl	TRP59	π- π Stacked
	Phenyl	TYR62	π- π Stacked
	Methoxy	TYR62	π- π Stacked
	Methoxy	HIS299	π- alkyl
<b>3</b> g	C=O	GLN63	Conventional H-bond (2.69 Å)
	Phenyl	TRP201	π- π Stacked
	Phenyl	TYR62	π- π Stacked
	Fluorine	ASP300	Halogen
	Fluorine	HIS299	Halogen
	Fluorine	ASP197	Halogen
3h	-C=O	GLN63	Conventional H-bond (2.20 Å)
	Phenyl	TRP59	π-π Stacked
	Methoxy	GLU233	Carbon Hydrogen Bond
	Phenyl	TYR62	π-π Stacked
3j	Oxygen	GLN63	Conventional H-bond (2.10 Å)
-	Phenyl	TRP59	π-π Stacked
	Phenyl	TYR62	π-π Stacked
	Methoxy	HIS305	π- alkyl
	Methoxy	TRP59	π- sigma
	Methoxy	TRP59	π- alkyl

**Table 3.** Docking interactions of synthesized compounds within the binding pocket of  $\alpha$ -amylase

The docked compounds 3a, 3e, 3g, 3h, and 3j were generally well suited to the binding site of  $\alpha$ amylase. With the imbedded amino acid residues, they produced a range of hydrogen bonds and hydrophobic interactions. The carbonyl moiety of the ligand and the associated phenyl group were found to have the strongest interactions. The active site residue GLN63 in compound 3a (Figure 1a) established a typical hydrogen bond with the carbonyl functional group's oxygen atom at a distance of 2.67 Å. The  $\pi$ - $\pi$  stack of the phenyl rings produced  $\pi$ -cations and  $\pi$ -anion with TRP59 and TYR62, respectively. This could be because the aromatic rings are planar, which forms an efficient conjugated  $\pi$ - $\pi$  system with the amino acid residue's active site. Additionally, in compound 3e (Figure 1b), the carbonyl carbon bonded to gln63 to create a typical hydrogen bond (2.30). The compound's methoxy group interacted with the TYR62 and HIS299 by  $\pi$ -  $\pi$  stacked and  $\pi$ - alkyl interactions, while the TRP59 and TYR62 created  $\pi$ -  $\pi$ stacked contacts with the phenyl ring. The carbonyl oxygen atom engaged in a typical hydrogen bonding interaction with GLN63 in the docked 3g derivative (Figure 1c) (2.69 Å). Additionally, the phenyl groups'  $\pi$  system created  $\pi$ - $\pi$  stacks with TYR62 and TRP201, respectively. Furthermore, a characteristic hydrogen bond (2.30) was formed between the carbonyl carbon and gln63 in compound 3e (Figure 1b). While the TRP59 and TYR62 formed  $\pi$ - $\pi$  stacked contacts with the phenyl ring, the compound's methoxy group interacted with the TYR62 and HIS299 through  $\pi$ -  $\pi$  stacked and  $\pi$ -alkyl interactions. The docked 3g derivative (Figure 1c) (2.69 Å) showed a typical hydrogen bonding contact between the carbonyl oxygen atom and GLN63. Furthermore, the  $\pi$  system of the phenyl groups produced  $\pi$ - $\pi$  stacks with TRP201 and TYR62, respectively.

# 3.4. Structure-Activity Relationship (SAR)

As far as we are aware, there is very little information available regarding the  $\alpha$ -amylase inhibitory activities of 2-benzylidene-1-indanone derivatives and their SAR (Figure 2). With an isopropyl group on

the benzene ring A, compounds 30 were just as potent as a carbose.  $\alpha$ -amylase inhibitory characteristics (34.5 and 35.5 µM) were dramatically reduced when OH groups (3b and 3c) were present at the *meta* and para positions. This suggests that the presence of hydroxyl groups at these sites was not well tolerated in the active site of the  $\alpha$ -amylase enzyme. Compound 3a's benzene ring A had hydroxyl groups at the *ortho* position, which demonstrated a strong  $\alpha$ -amylase inhibiting effect (17.7  $\mu$ M). Compound 3e is more effective and has a greater  $\alpha$ -amylase inhibitory potential (17.3  $\mu$ M) than compound 3a due to the presence of a chlorine atom at the *para* position on the benzene ring A. This suggests that the activity prefers a chlorine atom at this location and this is reported in literature which revealed that a significant amount of biologically active substances contains aromatic, heteroaromatic, or acyl substituents. <sup>26</sup> For instance, the presence of benzene-substituted and substituents comprising nitrogen, sulphur, and halogen have been observed to increase the biological activity of the initial chemical compounds. 26 With IC50 values of 19.0±4.6, 19.8±1.0, and 19.7±1.2 μM, respectively, the addition of fluorine, methoxy group, and bromine (3g, 3h, and 3j) also affects the activity. This indicates that the functional groups on benzene ring A that withhold electrons have a high tolerance. This is confirmed by Janse van Rensburg and co-workers reported that Improved affinity for the A1 and A2A receptors were demonstrated by the methoxysubstituted 2-benzylidene-1-indanone derivatives, which had a C4-OCH<sub>3</sub> group on ring A and *meta* (3') and *para* (4') dihydroxy substitutions on ring A of the benzylidene indanone scaffold.<sup>14</sup> Even though, there was reduced inhibitory  $\alpha$ -amylase activity when dimethoxy, trimethoxy, naphthyl, nitro, and methoxy groups were added to ring A in an ortho position. <sup>14</sup> However, by considering the electronic parameters of the groups to better understand the substituent effects, a preliminary correlation between Hammett sigma constants (σ) and experimental IC<sub>50</sub> values indicated that electron-withdrawing substituents (Cl, Br, F) generally enhanced activity, while electron-donating substituents (-OCH<sub>3</sub>, -OH in meta/para positions, -NO2) tended to decrease activity. Although a complete linear free-energy relationship (LFER) was not performed, these trends suggest that negative σ values (electron-donating) destabilize binding interactions, whereas positive σ values (electron-withdrawing) contribute to stronger affinity. Hydrophobic contributions also played a role, compound 30, with an isopropyl substituent, showed comparable activity to acarbose, suggesting that steric bulk in ring A can be tolerated with significant loss of binding affinity. Besides, derivatives containing multiple methoxy groups (dimethoxy, trimethoxy) or bulky aromatic substitutions (naphthyl) also showed reduced activity, likely due to steric hindrance within the binding site.<sup>14</sup>

Figure 2. A designed strategy for the SAR studies of derivatives

#### 3.5. Physicochemical, Drug Likeness and ADME Properties

In order for a molecule to be a powerful medication, it must sufficiently concentrate at its target location in the body and remain there in a bioactive form for the anticipated biologic events to take place. Considering that drug research entails evaluations of pharmacokinetic characteristics including absorption, distribution, metabolism, and excretion (ADME), computer models are legitimate substitutes for studies in this context. The Swiss ADME web tool offers free access to a collection of historical, reliable predictive models for the physicochemical characteristics, pharmacokinetics, and drug similarity of substances, as well as simple, effective inputs. <sup>22,31,32</sup> Using the Swiss ADME web tool, the ADME and drug likeness of substituted 2-benzylidene-1-indanone derivatives (3a–3p) were calculated; the results are shown in Tables 4-7.

Synthesis 2-benzylidene-1-indanone derivatives

Table 4. Physicochemical properties of the synthesised compounds

Compounds	Physicochemical properties							
	MW (g/mol) (<500)	Num. of Hea. Atom	Num. of Arom. Hea. atoms	Fractions Csp3	nHBD (≤5)	nHBA (≤10)	n-rot. B	
3a	236.3	18	12	0.06	1	2	1	
<b>3</b> b	236.3	18	12	0.06	1	2	1	
3c	236.3	18	12	0.06	1	2	1	
3d	254.7	18	12	0.06	1	1	0	
3e	254.7	18	12	0.06	1	1	0	
3f	289.6	19	12	0.06	1	1	0	
3g	238.3	18	12	0.06	1	2	0	
3h	250.2	19	12	0.12	2	2	0	
3i	299.1	18	12	0.06	1	1	0	
3j	280.3	21	12	0.17	3	3	0	
3k	280.3	21	12	0.17	3	3	0	
31	310.3	23	12	0.21	4	4	0	
3m	270.3	21	16	0.05	1	1	0	
3n	265.3	20	12	0.06	2	3	0	
30	262.4	20	12	0.21	2	1	0	
<b>3</b> p	250.3	19	12	0.12	2	2	0	
Acarbose	645.6				14	19	13	

**Table 5.** Lipophilicity properties of the synthesised compounds

Compounds		Lipophilicity								
	MR	TSPA	iLOG P	Consensus	ESOL	ESOL CLASS				
		(Å)		Log Po/w	Log S					
3a	71.1	37.3	2.4	3.1	-3.9	soluble				
<b>3</b> b	71.1	37.3	2.1	3.0	-3.9	soluble				
3c	71.1	37.3	2.2	3.0	-3.9	Soluble				
3d	74.1	17.0	2.7	4.0	-4.6	Molecule Soluble				
<b>3e</b>	74.1	17.0	2.8	4.0	-4.6	Molecule Soluble				
3f	79.1	17.0	115.5	4.5	-5.2	Molecule Soluble				
3g	69.1	17.1	2.7	3.8	-4.2	Molecule Soluble				
3h	75.6	26.3	2.8	3.5	-4.1	Molecule Soluble				
3i	76.8	17.1	2.9	4.1	-4.9	Molecule Soluble				
3j	82.0	35.5	3.1	3.4	-4.2	Molecule Soluble				
3k	82.0	35.5	3.1	3.4	-4.2	Molecule Soluble				
31	88.6	44.8	3.3	3.4	-4.2	Molecule Soluble				
3m	86.6	17.1	2.9	4.4	-5.2	Molecule Soluble				
3n	77.9	62.9	2.3	2.9	-4.1	Molecule Soluble				
30	83.7	17.1	3.2	4.4	-4.1	Molecule Soluble				
<b>3</b> p	75.6	26.3	2.7	3.45	-4.8	Molecule Soluble				
Acarbose			329.0	-7.4	47.6	Molecule Soluble				

The compounds' drug-likeness filters were evaluated for breaches of Lipinki's rule of five and compared to the suggested values. i) Lipinski filter: HBD $\leq$ 5, MLogP $\leq$ 4.15, MW $\leq$ 500, and HBA $\leq$ 10<sup>33</sup> ii) Ghose filter: -0.4 $\leq$ WlogP $\leq$ 5.6, 40 $\leq$ MR $\leq$ 130, 20 $\leq$ atoms $\leq$ 70, 160 $\leq$ MW $\leq$ 480<sup>34</sup> iii) RB $\leq$ 10, TPSA $\leq$ 140 Veber (GSK) filter<sup>35</sup> iv) Egan (Pharmacia) filters: TPSA $\leq$ 131.6, WLogP $\leq$ 5.88.<sup>36</sup> 200 $\leq$ MW $\leq$ 600, -2 $\leq$ XLogP $\leq$ 5, TPSA $\leq$ 157, HBD $\leq$ 5, RB $\leq$ 15, number of rings  $\leq$ 7, number of carbons >4, number of heteroatoms  $\leq$ 1 are the parameters for the Muegge (Bayer) filter.<sup>37</sup> All compounds satisfied Veber's rule, with rotatable bond counts <10 and TPSA values under 140 Ų, suggesting favorable oral bioavailability.

Similarly, according to Egan's rule, the LogP values (<5.88) and TPSA values (<131 Ų) place the compounds within the acceptable range for intestinal absorption. Moreover, Muegge's filter confirmed that all derivatives lie within the drug-like chemical space without any violations, further supporting their potential as promising drug-like candidates. Most of the compounds did not break the Veber, Egan, and Muegge rules, but none break the Lipinski and Ghose rule. In conclusion, substituted 2-benzylidene-1-indanone derivatives (3a–3p) demonstrated acceptable ADME values and satisfied the drug likeness requirements.<sup>38</sup>

**Table 6.** Pharmacokinetics properties of the synthesised compounds

Compounds	GIA	BBB	P-gp subs	CYP1	CYP2C	CYP2	CYP2	CYP3	Log Kp
•			<b>.</b>	<b>A2</b>	19	<b>C9</b>	<b>D6</b>	<b>A4</b>	(cm/s)
3a	High	Yes	No	Yes	Yes	No	No	No	-5.3
<b>3</b> b	High	Yes	No	Yes	Yes	No	No	No	-5.3
3c	High	Yes	No	Yes	Yes	No	No	No	-5.3
3d	High	Yes	No	Yes	Yes	No	No	No	-4.7
3e	High	Yes	No	Yes	Yes	No	No	No	-4.7
3f	High	Yes	No	Yes	Yes	Yes	No	No	-4.5
3g	High	Yes	No	Yes	Yes	No	No	No	-4.9
3h	High	Yes	No	Yes	Yes	No	Yes	No	-5.2
3i	High	Yes	No	Yes	Yes	Yes	No	No	-4.9
3j	High	Yes	No	Yes	Yes	Yes	Yes	Yes	-5.4
3k	High	Yes	No	Yes	Yes	Yes	Yes	Yes	-5.4
31	High	Yes	No	Yes	Yes	Yes	Yes	Yes	-5.6
3m	High	Yes	No	Yes	Yes	No	No	No	-4.4
3n	High	Yes	No	Yes	Yes	Yes	No	No	-5.4
30	High	Yes	No	No	No	No	Yes	No	-4.4
3p	High	Yes	No	Yes	Yes	No	Yes	No	-5.2
Acarbose	No	No	Yes	No	No	No	No	No	-16.5

**Table 7.** Drug-likeness of the synthesised compounds

S. No.	Compounds	Lipinski	Ghose	Veber	Egan	Muegge	Bioavailability
							score
1.	3a	Yes	Yes	Yes	Yes	Yes	0.55
2.	<b>3</b> b	Yes	Yes	Yes	Yes	Yes	0.55
3.	3c	Yes	Yes	Yes	Yes	Yes	0.55
4.	3d	Yes	Yes	Yes	Yes	No	0.55
5.	<b>3e</b>	Yes	Yes	Yes	Yes	No	0.55
6.	3f	Yes	Yes	Yes	Yes	No	0.55
7.	3g	Yes	Yes	Yes	Yes	No	0.55
8.	3h	Yes	Yes	Yes	Yes	Yes	0.55
9.	3i	Yes	Yes	Yes	Yes	Yes	0.55
10.	3j	Yes	Yes	Yes	Yes	Yes	0.55
11.	3k	Yes	Yes	Yes	Yes	Yes	0.55
12.	31	Yes	Yes	Yes	Yes	Yes	0.55
13.	3m	Yes	Yes	Yes	Yes	No	0.55
14.	3n	Yes	Yes	Yes	Yes	Yes	0.55
15.	<b>3</b> 0	Yes	Yes	Yes	Yes	Yes	0.55
16.	<b>3</b> p	Yes	Yes	Yes	Yes	Yes	0.55
17.	Acarbose	NO	NO	YES	NO	NO	NO

#### 4. Conclusion

In this study, a series of substituted 2-benzylidene-1-indanone derivatives (3a-3p) were successfully synthesized via a condensation reaction using substituted 2-benzaldehydes (2) and 1-indanone (1). The structures of the synthesized compounds were confirmed through HRMS, FTIR, <sup>1</sup>H NMR, and <sup>13</sup>C NMR analyses. Their potential as  $\alpha$ -amylase inhibitors was evaluated using *in vitro* assays supported by computational molecular docking studies. Among the derivatives, compounds 3a, 3e, 3g, 3h, and 3j exhibited significant inhibitory activity compared to the standard drug acarbose, with

compounds 3a and 3e showing the strongest effects due to hydroxyl and chlorine substitutions at the *para* position. Molecular docking results correlated well with experimental findings, as these active compounds demonstrated low docking score and favorable orientations within the  $\alpha$ -amylase active site (PDB ID: 2QV4). Structure–activity relationship (SAR) analysis revealed that an *ortho*-positioned hydroxyl group (compound 3a) enhanced inhibitory activity, while chlorine (3e), fluorine (3e), methoxy (3e), and bromine (3e) substitutions further improved potency. Conversely, dimethoxy, trimethoxy, naphthyl, nitro, and *ortho*-methoxy substitutions reduced inhibitory effects. Additionally, computational ADME profiling using SwissADME confirmed that most derivatives exhibited desirable pharmacokinetic properties and complied with Lipinski's and Ghose's drug-likeness rules, although some deviations were observed in Veber, Egan, and Muegge filters. Overall, the substituted 2-benzylidene-1-indanone derivatives, particularly compounds 3a and 3e, show promising potential as lead candidates for the development of novel  $\alpha$ -amylase inhibitors for antidiabetic therapy.

#### Acknowledgements

The authors would like to acknowledge the financial support from the Ministry of Higher Education Malaysia (MOHE) under the Fundamental Grant Research Scheme (FRGS)-FRGS/1/2023/STG04/USM/02/3. The authors sincerely thank University Sains Malaysia (USM) and the NPSO Laboratory for the facilities used in this research work.

# **Supporting Information**

Supporting information accompanies this paper on <a href="http://www.acgpubs.org/journal/organic-communications">http://www.acgpubs.org/journal/organic-communications</a>



Selvakumar Sabapathi: 0009-0003-1457-3686

Babai Mahdi: 0000-0001-8565-0595

Mohamad Hafizi Abu Bakar: <u>0000-0001-8064-695X</u> Andrey A. Mikhaylov: <u>0000-000</u>1-9433-9141

Mohammad Tasyriq Che Omar: 0000-0002-1294-7520

Azeana Zahari: 0000-0002-5279-0169

S. Yaallini Sukumaran: <u>0009-0009-4183-6377</u> Mohamad Nurul Azmi: <u>0000-0002-2447-0897</u>

#### References

- [1] Babai, M.; Azmi, M. N.; Lacksany, P.; Muhammad Solehin, A. G.; Mohamad Hafizi, A. B.; Mohammad Tasyriq, C. O.; Unang, S. Synthesis of *ortho*-carboxamidostilbene analogues and their antidiabetic activities through *in vitro* and *in silico* approaches. *Organic. Comm.* **2024**, *17*(1), 8-22.
- [2] Rishi, R.; Claude, K.; Kavita, M. K.; Sriram, N.; Avery, H.; Andrew, D.; Hsin-Chieh, Y.; Felicia, H. B.; Mariana, L. Prevalence of self-reported sleep duration and sleep habits in type 2 diabetes patients in South Trinidad. *J. Epidemiol. Glob. Health.* **2015**, *5*, S35–S43.
- [3] Shreenivas, R. D.; Mallikarjun, W.; Prasad, V. M.; Prabhu, C. J. Design, synthesis, *in silico* studies, and antidiabetic activity of several sulphanilamide incorporated 2,3-disubstituted thiazolidin-4-ones, *Rev. Colomb. Quim.* **2023**, *51*(3), 3-13.
- [4] Fettach, S.; Thari, F. Z.; Hafidi, Z.; Karrouchi, K.; Bouathmany, K.; Cherrah, Y.; Achouri, M. El; Benbacer, L.; Mzibri, M. El.; Sefrioui, H.; Bougrin, K.; Faouzi, M. E. A. Biological, toxicological and molecular docking evaluations of isoxazoline-thiazolidine-2,4-dione analogues as new class of antihyperglycaemic agents. *J. Biomol. Struct. Dyn.* **2023**, *41*(3), 1072–1084.
- [5] Shafique, K.; Farrukh, A.; Mahmood Ali, T.; Qasim, S.; Jafri, L.; Abd-Rabboh, H. S. M.; AL-Anazy, M. M.; Kalsoom, S. Designing click one-pot synthesis and antidiabetic studies of 1,2,3-triazole derivatives. *Molecules* **2023**, *28*(7), 3104-3120.
- [6] Zeka, K.; Arroo, R. R. J.; Hasa, D.; Beresford, K. J. M.; Ruparelia, K. C. New resveratrol analogues for potential use in diabetes and cancer. *Biomed. J. Sci. Tech. Res.* **2018**, *6*(2), 5201-5206.

- [7] Khan, I.; Rehman, W.; Rahim, F.; Hussain, R.; Khan, S.; Rasheed, L.; Alanazi, M. M.; Alanazi, A. S.; Abdellattif, M. H. Synthesis and *in vitro* α-amylase and α-glucosidase dual inhibitory activities of 1,2,4-triazole-bearing bis-hydrazone derivatives and their molecular docking study. *ACS Omega* **2023**, 8(25), 22508–22522.
- [8] International Diabetes Federation IDF Diabetes Atlas Diabetes Facts and Figures; Available online: <a href="http://www.idf.org/about-diabetes/facts-figures">http://www.idf.org/about-diabetes/facts-figures</a>.
- [9] Institute for Public Health. National Health and Morbidity Survey 2015 (NHMS 2015). Vol. II: Non-communicable diseases, risk factors & other health problems. *Minist. Health Malays*, **2015**, *2*, 185-186.
- [10] Gabrial, A. G.; Thomas, I. G. R.; Sarah, E. L.; Fei, W.; Stephen, C.; Carine, de B.; Kim, C. D.; Dianna, J, M.; Jayanthi, M.; Trevor, J. O.; Priyanka, R.; Graham, D. O. Global incidence, prevalence, and mortality of type 1 diabetes in 2021 with projection to 2040: A modelling study. *Lancet Diabetes Endocrinol.* **2022**, *10*(10), 741-760.
- [11] Alotaibi, A.; Perry, L.; Gholizadeh, L.; Al-Ganmi, A. Incidence and prevalence rates of diabetes mellitus in Saudi Arabia: An overview. *J. Epidemiol. Glob. Health.* **2017**, *7*, 211–218.
- [12] Lone, S.; Lone, K.; Khan, S.; Pampori, R. A. Assessment of metabolic syndrome in Kashmiri population with type 2 diabetes employing the standard criteria's given by WHO, NCEPATP III and IDF. *J. Epidemiol. Glob. Health.* **2017**, *7*, 235–239.
- [13] IDF Diabetes Atlas 10<sup>th</sup> edition **2021**.
- [14] Sanni, O.; Terre'Blanche, G. Dual A1 and A2A adenosine receptor antagonists, methoxy substituted 2-benzylidene-1-indanone, suppresses intestinal postprandial glucose and attenuates hyperglycaemia in fructose-streptozotocin diabetic rats. *BMC Endocr. Disord.* **2023**, *23*, 97.
- [15] Mohamad, N.; Phua, Y. H.; Abu Bakar, M. H.; Che Omar, M. T.; Wahab, H. A.; Supratman, U.; Awang, K.; Azmi, M. N. Synthesis, biological evaluation of *ortho*-carboxamidostilbenes as potential inhibitors of hyperglycaemic enzymes, and molecular docking study. *J. Mol. Struct.* **2021**, *1245*(*21*), 131007.
- [16] Mahanta, T. G.; Joshi, R.; Mahanta, B. N.; Xavier, D. Prevalence of modifiable cardiovascular risk factors among tea garden and general population in Dibrugarh, Assam, *India. J. Epidemiol. Glob. Health.* 2013, 3, 147–156.
- [17] Oluyombo, R.; Olamoyegun, M. A.; Olaifa, O.; Iwuala, S. O.; Babatunde, O. A. Cardiovascular risk factors in semi-urban communities in southwest Nigeria: Patterns and prevalence. *J. Epidemiol. Glob. Health.* **2015**, *5*, 167–174.
- [18] Movahed, A.; Nabipour, I.; Lieben Louis, X.; Thandapilly, S. J.; Yu, L.; Kalantarhormozi, M.; Rekabpour, S. J.; Netticadan, T. Antihyperglycemic effects of short-term resveratrol supplementation in type 2 diabetic patients. *Evid. Based. Complement. Alternat. Med.* **2013**, *13*, 1-11.
- [19] Bommer, C.; Sagalova, V.; Heesemann, E.; Manne-Goehler, J.; Atun, R.; Bärnighausen, T.; Davies, J.; Vollmer, S. Global economic burden of diabetes in adults: projections from 2015 to 2030. *Diabetes Care* **2018**, *41*(5), 963–970.
- [20] Farhood, H. B.; Al- Salih, R. M.; Radhi, M. N. Clinical studies to evaluate pancreatic functions in the patients of type 2 diabetes mellitus, *IJIAS*, **2014**, *7*(*I*), 413-420.
- [21] Abu Bakar, M. H.; Lee, P. Y.; Azmi, M. N.; Lotfiamir, N. S.; Faris Mohamad, M. S.; Nor Shahril, N. S.; Shariff, K. A.; Ya'akob, H.; Awang, K.; Litaudon, M. *In vitro* anti hyperglycaemic, antioxidant activities and intestinal glucose uptake evaluation of *Endiandra kingiana* extracts. *Biocatal. Agric. Biotechnol* **2020**, *25*, 1-11.
- [22] Babai, M.; Mohamad Hafizi, A. B.; Mohamad Tasyriq, C. O.; Azeana, Z.; Mohammad. M. I.; Andrey, A. M.; Azmi, M. N. Synthesis of *para*-carboxamidostilbene derivatives as antihyperglycemia agents and their *in silico* ADMET and molecular docking studies *ChemistrySelect*, **2024**, *9*, e202402433.
- [23] Phongphane, L.; Mohd Radzuan, S. N.; Abu Bakar, M. H.; Che Omar, M. T.; Supratman, U.; Harneti, D.; A. Wahab, H.; Azmi, M. N. Synthesis, biological evaluation, and molecular modelling of novel quinoxaline-isoxazole hybrid as anti-hyperglycemic. *Comput. Biol. Chem.* 2023, 106, 107938
- [24] Garrett, M. M.; Ruth, H.; William, L.; Michel, F. S.; Richard, K. B.; David, S. G.; Arthur, J. O. AutoDock4 and AutoDockTools4: Automated docking with selective receptor flexibility. *J. Comput. Chem.*, **2009**, 30(16), 2785-2791.
- [25] Mohd Radzuan, S. N.; Phongphane, L.; Abu Bakar, M. H.; Che Omar, M. T.; Nor Shahril, N. S.; Supratman, U.; Azmi, M. N. Synthesis, biological activities, and evaluation molecular docking-dynamics studies of new phenyl isoxazole quinoxalin-2-amine hybrids as potential α-amylase and α-glucosidase inhibitors RSC Adv. 2024, 14(11), 7684-7698.

- [26] Kawsar, S. A. M.; Hosen, M. H.; El Bakri, Y.; Ahmad, S., Affi S. T.; Goumri-Said S. (2022) *In silico* approach for potential antimicrobial agents through antiviral, molecular docking, molecular dynamics, pharmacokinetic and bioactivity predictions of galactopyranoside derivatives, *Arab J. Basic Appl. Sci.* **2022**, 291, 99-112.
- [27] Zeleke, D.; Eswaramoorthy, R.; Belay, Z.; Melaku, Y. Synthesis and antibacterial, antioxidant, and molecular docking analysis of some novel quinoline derivatives. *J. Chem* **2020**, *20*, 1324096.
- [28] Al-Radadi, N. S.; Zayed, E. M.; Mohamed, G. G.; Abd El Salam, H. A. Synthesis, spectroscopic characterization, molecular docking, and evaluation of antibacterial potential of transition metal complexes obtained using triazole chelating ligand. *J. Chem.* **2020**, *20*, 1548641.
- [29] Antoine, D.; Olivier, M.; Vincent, Z. SwissADME: A free web tool to evaluate pharmacokinetics, drug-likeness, and medicinal chemistry friendliness of small molecules. *Sci. Rep.* **2017**, 7(1), 42717
- [30] Altay M. Acarbose is again on the stage. World J. Diabetes, 2022, 13(1), 1–4.
- [31] Akter, N.; Bourougaa, L.; Ouassaf, M.; Bhowmic, R. C.; Kabir M. U.; Bhat, A. J.; Ahmed, S.; Sarkar M.A. Kawsar S. M. A. Molecular docking, ADME-Tox, DFT and molecular dynamics simulation of butyroyl glucopyranoside derivatives against DNA gyrase inhibitors as antimicrobial agents, *J. Mol. Struct.* **2021**, 1307, 137930.
- [32] Chalkha, M.; Chebbac, K.; Nour, H.; Nakkabi, A.; El-Moussaoui, A.; Tüzün, B.; Bourhia, M.; Chtita, S; Bakhouch, M.; Laaroussi, H.; Sarkar M.A. Kawsar, S.M,A.; Hadda, T.; Al Houari, G.; Augustyniak, M.; Aboul-Soud, M. A.M.; El Yazidi, M. *In vitro* and *in silico* evaluation of the antimicrobial and antioxidant activities of spiropyrazoline oxindole *congeners Arab, J. Chem.* **2023**, *17*, 105465.
- [33] Christopher, A. L.; Franco. L.; Beryl, W. D.; Paul. J. F. Experimental and computational approaches to estimate solubility and permeability in drug discovery and development settings. *Adv. Drug Deliv. Rev.*, **1997**, 23(1-3), 3-25.
- [34] Arup, K. G.; Vellarkad, N. V.; John, J. W. Knowledge-based approach in designing combinatorial or medicinal chemistry libraries for drug discovery. 1. A qualitative and quantitative characterization of known drug databases. *J. Comb. Chem.* **1999**, *I*(*I*), 55-68.
- [35] Daniel, F. V.; Stephen, R. J.; Hung-Yuan, C.; Brian, R. S.; Keith, W. W.; Kenneth, D. K. Molecular properties that influence the oral bioavailability of drug candidates. *J. Med. Chem.* **2002**, *45*(*12*) 2615-2623.
- [36] William, J. E.; Kenneth, M. M.; John, J. B. Prediction of drug absorption using multivariate statistics (2000). J. Med. Chem. 2000, 43(21), 3867-3877.
- [37] Ingo, M.; Sarah, L. H.; David, B. Simple selection criteria for drug-like chemical matter. *J. Med. Chem.* **2001**, 44(12), 1841-1846.
- [38] Shreenivas, D.; Mallikarjun, W.; Prasad V. M.; Prabhu, C, J. Design, synthesis, *in silico* studies, and antidiabetic activity of several sulfanilamide incorporated 2,3-disubstituted thiazolidin-4-ones *Rev. Colomb. Quim*, **2022**, *51*(3), 3-13.

ACG
publications
© 2025ACG Publications